2.4 Mesoscale Convective Systems Crossing the Appalachian Mountains

Casey E. Letkewicz* and Matthew D. Parker
North Carolina State University, Raleigh, North Carolina

1. INTRODUCTION

Mesoscale convective systems (MCSs) have been the subject of numerous observational and numerical modeling studies due to their numerous potential hazards (i.e. flooding, severe winds, hail, and tornadoes) to both life and property. In order to better anticipate and forecast these impacts, past research has emphasized understanding the most fundamental dynamics of these systems, often neglecting other higher order complications such as environmental heteorogeneity or terrain. However, MCSs are not limited to areas of negligible topography, and recent research has begun examining the impact of orography on organized convective systems (Frame and Markowski 2006, Reeves and Lin 2007, Keighton et al. 2007).

Forecasting MCS maintenance presents a unique forecasting problem for operational meteorologists in the eastern portion of the United States due to the influence of the Appalachian Mountains. At times, MCSs are able to cross the mountains and produce severe weather in the lee, while at other times these systems instead dissipate upon encountering the terrain. Keighton et al. (2007) recently conducted an observation-based study that examined severe MCSs interacting with the Appalachians in more detail, finding that the ability of an MCS to cross the mountains (i.e. produce severe weather in the lee) was strongly dependent upon diurnal heating. Most cases categorized as "noncrossing" reached the western slopes or dissipated to the west during the overnight and morning hours while "crossing" cases tended to encounter the mountains during peak heating. Several other factors can complicate the continuation or dissipation of MCSs, includding blocking or modification of system-generated cold pools by the terrain, variations in instability due to differences in elevation, slope flows driven by diurnal heating or large-scale flow regimes, and even cold-air damming (Keighton et al. 2007). Frame and Markowski (2006) examined these systems in an idealized modeling framework, and found that squall lines traversing terrain went through a cycle of orographic enhancement on the upslope side, weakening, and subsequent restrengthening as the cool outflow air pooled at the base of the mountain downstream to form a hydraulic jump.

In light of these past studies, there still exists a need to not only differentiate between crossing and noncrossing MCS environments but also to understand the key processes at work which impact the ability of an MCS to cross the Appalachian Mountains. Accomplishing this goal is attained through analysis of observations in addition to idealized modeling simulations. The aim of this study is to aid forecasters in identifying typical environments of each case type and serve as a guide to understanding these systems better.

Section 2 will discuss the key observational findings; Section 3 will provide a brief overview of the idealized modeling results, while Section 4 will present conclusions and future work.

* *Corresponding author address:* Casey E. Letkewicz, Department of Marine, Earth, & Atmospheric Sciences, North Carolina State University, Campus Box 8208, Raleigh, NC 27695–8208. E-mail: celetkew@ncsu.edu

2. OBSERVATIONS

a. *Data and Methods*

A random sampling of 20 crossing and 20 noncrossing cases were chosen from the Keighton et al. (2007) database of MCSs in the Appalachian region that occurred between 2000 and 2006. These systems were categorized based on whether or not they were able to produce severe weather reports in the lee of the Appalachians. Note that *all* cases were severe west of the Appalachians. Therefore, "crossing" cases were able to produce severe reports on the eastern side of the barrier while "noncrossing" cases did not produce any severe reports east of the Blue Ridge (Figure 1). Noncrossing events also typically did not survive for long as non-severe convection east of the mountains. Please see Keighton et al. (2007) for complete details on their method of categorization.

The background environments of these cases were analyzed using operational radiosonde data. Two soundings were chosen for each case: one to represent the upstream environment west of the mountains and one to represent the downstream environment east of the mountains. The selections were based on the soundings that best represented the MCSs' inflow environments. At times this determination was difficult due to the spatial and temporal sparseness of the data, yet suitable soundings were found for each case. In order to obtain as accurate a representation of the low-level inflow environment as possible, the surface conditions of each sounding (temperature, dewpoint, relative humidity, wind speed and direction) were modified using a nearby surface observation from within the hour before MCS passage.

After modifying the soundings, numerous thermodynamic and kinematic parameters were calculated, the details of which (including the list of parameters) can be found in the Appendix. Once the parameter values were obtained, statistical analysis was performed in order to determine the extent to which crossing and noncrossing environments were different. The Monte Carlo method, chosen for its lack of assumptions about the distribution of the data, was applied to each parameter. By repeatedly randomly sampling and grouping the data, p-values were determined, representing the probability that the difference between groups is due to random sampling alone. Thus, a "low" p-value (for example, less than or equal to 0.05) is representative of a parameter which is significantly different between crossing and noncrossing cases. The subsequent analyses are therefore focused on the parameters with the lowest p-values.

b. *Results*

Through examination of composite soundings and wind profiles, it is clear that greater differences between crossing and noncrossing cases lie in the downstream environment compared to the upstream environment. Figure 2 reveals only a few subtle differences between crossing and noncrossing cases in the upstream environment, particularly in the moisture profile. Conversely, Figure 3 illustrates more noticeable differences between case types within the downstream environment. Specifically, crossing MCS environments had warmer temperatures, a higher moisture content, and a steeper low-level lapse rate, which would entail much higher instability. The wind profiles for all of the cases (specifically the mountain-perpendicular component which directly interacts with the terrain) also indicate fewer differences in the upstream environment (Figure 4) than the downstream environment (Figure 5), though both show a rather wide distribution and overlap of the profiles.

A comparison of Tables 1 and 2 confirms what was illustrated in Figures 2 through 5, that the downstream environment is much more discriminatory that the upstream environment, since there are numerous downstream parameters with a low ($\leq$ 0.05) p-value compared to only one in the upstream environment. This finding makes sense, given that both crossing and noncrossing MCSs were severe upstream of the Appalachians and thus should have comparable environments. This comparison also suggests that the environment that the MCS is moving into is more important for its maintenance than the one in which it developed. Nonetheless, DCAPE was the parameter that best separated crossing and noncrossing MCSs in the upstream environment. Crossing cases on average contained higher amounts of DCAPE, which can be associated with the potential for stronger cold pools (i.e. more evaporational cooling).

In the downstream environment, many of the discriminatory parameters were linked to the ambient stability. This is unsurprising, given the large low-level differences in temperature and moisture between case types in Figure 3. Notably, east of the mountains the environment tended to be quite a bit more unstable for crossing than noncrossing cases, with nearly 2000 J/kg more CAPE for the surface-based (SBCAPE) and most unstable parcels (MUCAPE). This finding is consistent with Keighton et al. (2007)'s discovery that most crossing MCSs occur during the peak of daytime heating (ie. when there is the greatest amount of instability). However, we did find that CAPE was larger for crossing cases and separated the cases well no matter the time of day that they occurred (not shown). Crossing cases also tended to have higher surface θ, θ_e, and q_v,which also coincide with greater instability. Notably, these surface parameters were well-correlated (~0.8) with SBCAPE. The surface to 500 mb θ_e difference's significance was mainly attributable to the surface θ_e value, given their near-perfect correlation of 0.94. The steeper 0-3 km lapse rate separating crossing cases from noncrossing cases also contained a robust link to SBCAPE (~0.6). The last noteworthy thermodynamic parameter was MUCIN, which was on average smaller (i.e. less inhibition) for MCSs able to traverse the terrain. This parameter appears to add skill because it was not found to be strongly correlated to other variables. Overall, crossing cases tended to have thermodynamic environments in the lee of the mountains that were more favorable for convection. Since many of these parameters were significantly correlated to one another, however, CAPE is revealed as the most important thermodynamic factor.

In addition to instability, wind speed and shear vector magnitudes in the lee of the mountains were also found to separate crossing and noncrossing MCS environments, despite the wide distribution and overlap of profiles in Figure 5. The most useful parameters included maximum bulk shear (see the Appendix for its definition), 0-3 km shear, 3-12 km mean wind speed, 0-6 km shear, and the mountain-perpendicular component of the 0-3 km shear and the mean 3-12 km wind speed. Notably, the average for each of these parameters was *smaller* for crossers than noncrossers. Higher shear is generally beneficial (to an extent) for convective organization and MCS maintenance (Rotunno et al. 1988, Coniglio et al. 2007), thus it is perplexing to find the opposite observed. It has been observed ancedotally and noted in an idealized setting (Frame and Markowski 2006) that MCSs weaken while traversing the barrier, in part because their cold pools are partially blocked. Thus, smaller shear values downstream may provide a better balance with a weakened cold pool (i.e. weaker baroclinc vorticity generated from the cold pool balanced with the weaker vorticity from the environmental shear; Rotunno et al. 1988). Alternatively, the finding that crossing cases had a weaker mean wind could be explained by considering slope flows induced by the ambient wind. In a westerly wind regime, upslope flow is located on the windward side of the mountain acting to enhance the convection, while downslope flow is found in the lee, leading to convection being suppressed. A weaker mean wind could thus be beneficial for squall lines by allowing for less sinking motion downstream of the mountain. However, it is also important to keep in mind that mean wind and shear are inherently correlated with each other. Thus, both the effects of slope flows and the balance between cold pool and shear may be working in tandem to promote or inhibit a successful propagation over the barrier. These hypotheses were tested using numerical simulations, discussed in the next section.

3. IDEALIZED MODELING

a. *Model & Experimental Design*

In light of the unexpected observation of comparatively weaker shear and mean wind in the lee for crossing cases, idealized simulations were used to evaluate their contribution to the maintainence of a squall line as it traverses terrain. This study employed Version 1.11 of the Bryan Cloud Model (CM1; Bryan and Fritsch 2002), using a horizontal grid spacing of 1 km and a vertical grid stretched from 150 m at the model surface to 500 m aloft. The periodic y-dimension was 60 km in extent; the across-line x-dimension was nominally 600 km, although this was increased for the faster-moving squall line simulations. Convection was initiated using a line thermal with a θ' of +4 K and the homogeneous base state thermodynamic environment was specified by the idealized Weisman and Klemp (1982) thermodynamic profile. The squall line was allowed to evolve and mature for three hours before its cold pool reached the base of the mountain. The dimensions of the mountain remained constant, a Gaussian bell-shaped hill with a half width of 50 km and a height of 1 km, roughly approximating the dimensions of the Appalachian Mountains. The mountain was infinitely long in the y-direction.

The five wind profiles that were tested are illustrated in Figure 6, and are similar to those used in other idealized simulations of squall lines (e.g. Rotunno et al. 1988, Frame and Markowski 2006). The first set of sensitivity tests increased and decreased the mean wind by 5 ms^{-1}, while the second set increased and decreased the low-level shear by 5 ms^{-1}.

b. *Results*

After testing these profiles, it was found that all of the squall lines were able to successfully traverse the terrain and undergo a period of orographic enhancement, suppression, and convective reinvigoration in the lee, akin to the process described by Frame and Markowski (2006; Figure 7). However, Figure 7 does illustrate that the intensity of the simulated reflectivity and the distance from the mountain peak at which it becomes restrengthened is modulated by changes to the wind profile. Thus the wind profile appears to *modulate* the crossing process, but does not solely determine the ability of an MCS to successfully traverse terrain. In addition to the process described by Frame and Markowski (2006), the simulations showed that orographic gravity waves also contributed to convective reintensification in the lee. As illustrated by the control run, the gravity waves acted first to develop new convection out ahead of the cold pool, and then once the squall line's cold pool reached the wave's zone of ascent approximately 260 min into the simulation (located at x=40 to 60 km east of the mountain peak), the updraft was significantly restrengthened (Figure 8). The magnitude of these gravity waves was dependent upon the strength of the mean wind; thus, for the wind profiles which had a weaker mean wind, the hydraulic jump mechanism was the primary contributor to the system's reintensification in the lee, while for the wind profiles with a stronger mean wind, gravity waves played a larger role in system restrengthening. Nonetheless, each change to the wind profile produced a crossing MCS as a result of the hydraulic jump in the cold pool and orographic gravity waves acting to reinvigorate the convection downstream.

It is also important to reemphasize that these simulations utilized the Weisman and Klemp (1982) sounding, which is an extremely favorable environment for the maintenance of convection (i.e. high CAPE and low CIN). Based on the observed soundings (Section 2), it appears that the temperature and moisture profiles play a more important role in the maintenance of these squall lines, rather than the wind profiles. The testing of less favorable thermodynamic environments should be performed in future studies.

4. CONCLUSIONS & FUTURE WORK

Examination of 20 crossing and 20 noncrossing MCSs encountering the Appalachian Mountains revealed that crossing cases tended to be characterized by higher CAPE and lower CIN, in addition to a weaker mean wind and shear in the downstream environment. While the presence of more instability and less inhibition was relatively straightforward, the slower mean wind and less shear was not as easy to understand. Two hypotheses attempted to explain the apparent benefit of having less shear and a weaker mean wind: one applied the theory put forth by Rotunno et al. (1988) concerning the maintenance of squall lines, believing that weaker shear would provide a better balanced with a weakened cold pool in the lee, while the other suggested that a slower mean wind would result in weaker downslope flow, and thus less convective suppression in the lee.

Through tests using several variations of the wind profile in an idealized setting it was found that, when there is a suitably favorable thermodynamic sounding, convective systems show little sensitivity to changes in the wind profile in terms of their maintenance. However, the systems did exhibit changes in intensity and the degree to which they were suppressed in the lee. Terrain-induced gravity waves also significantly contributed to the system's renewal downstream of the mountain, in addition to the hydraulic jump of the cold pool. Given the overall importance of instability for convective maintenance, forecasters are encouraged to take into account the thermodynamic environment (i.e. CAPE and CIN) in the lee of the mountains first and foremost. However, forecasters should also be aware of the wind profile and its potential effects, particularly slope flows which impact orographic enhancement and suppression.

A goal of future studies should be to understand the processes which occur in noncrossing MCSs, particularly since this study was unable to produce one using the idealized simulations. The use of less favorable thermodynamic soundings and more complex terrain geometries are avenues which should be explored in order to achieve greater understanding of these systems which encounter terrain.

Acknowledgements. The research reported here is supported by the National Science Foundation under Grant ATM-0552154 and by National Oceanic and Atmospheric Administration's Collaborative Science, Technology and Applied Research (CSTAR) program Award NA07NWS4680002. Thanks also go to the Convective Storms Group at NC State University for their assistance and feedback.

References

Bryan, G. H., and M. J. Fritsch, 2002: A benchmark simulation for moist nonhydrostatic numerical models. *Mon. Wea. Rev.*, **128**, 3941–3961.

Coniglio, M. C., H. E. Brooks, S. J. Weiss, and S. F. Corfidi, 2007: Forecasting the maintenance of quasi-linear mesoscale convective systems. *Wea. Forecasting*, **22**, 556–570.

Frame, J., and P. Markowski, 2006: The interaction of simulated squall lines with idealized mountain ridges. *Mon. Wea. Rev.*, **134**, 1919–1941.

Keighton, S., J. Jackson, J. Guyer, and J. Peters, 2007: A preliminary analysis of severe quasi-linear mesoscale convective systems crossing the Appalachians. Preprints, *22nd Conference on Weather Analysis and Forecasting*, Park City, UT, Amer. Meteor. Soc.

Reeves, H. D., and Y.-L. Lin, 2007: The effects of a mountain on the propagation of a preexisting convective system for blocked and unblocked flow regimes. *J. Atmos. Sci.*, **64**, 2401–2421.

Rotunno, R., J. B. Klemp, and M. L. Weisman, 1988: A theory for strong, long–lived squall lines. *J. Atmos. Sci.*, **45**, 463–485.

Weisman, M. L., and J. B. Klemp, 1982: The dependence of numerically simulated convective storms on vertical wind shear and buoyancy. *Mon. Wea. Rev.*, **110**, 504–520.

Appendix

Parameters computed for this study were chosen based upon past research (e.g. Coniglio et al. 2007) and personal communications with forecasters from the Raleigh and Blacksburg National Weather Service forecast offices and also the Storm Prediction Center. These parameters include Convective Available Potential Energy (CAPE) and Convective Inhibition (CIN) of the surface parcel, the most unstable parcel (MUCAPE & MUCIN), and the 0-1 km mixed layer parcel (MLCAPE & MLCIN); downdraft CAPE (DCAPE), heights of the Lifting Condensation Level (LCL) and Level of Free Convection (LFC), the shear vector magnitudes over the 0-1 km, 0-3 km, 0-6, 3-12 km, and 2-8 km layers; maximum bulk shear (defined as the maximum shear vector magnitude between 0-1 km and 6-10 km); 1 km wind speed, 3-12 km mean wind speed, 0-3 and 3-8 km lapse rate, 850 mb dewpoint, θ, and θ_e; surface to 500 mb difference in θ_e, precipitable water, and surface properties such as θ, θ_e, mixing ratio, and also the north-south component of the wind. Note that CIN values were only averaged if they were accompanied by CAPE values greater than zero. Each shear and wind variable was also calculated for the mountain-perpendicular component of the wind.

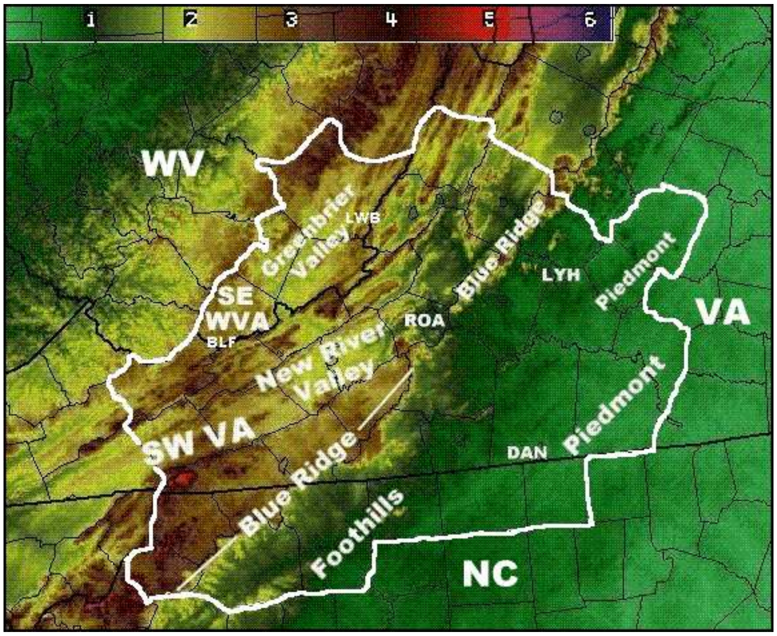

Figure 1: Topographic map (scale is in thousands of feet) denoting the geographical areas within the Blacksburg, Virginia Weather Forecasting Office county warning area (white border). Note that the Blacksburg CWA is only a portion of the entire study domain (see Keighton et al. 2007).

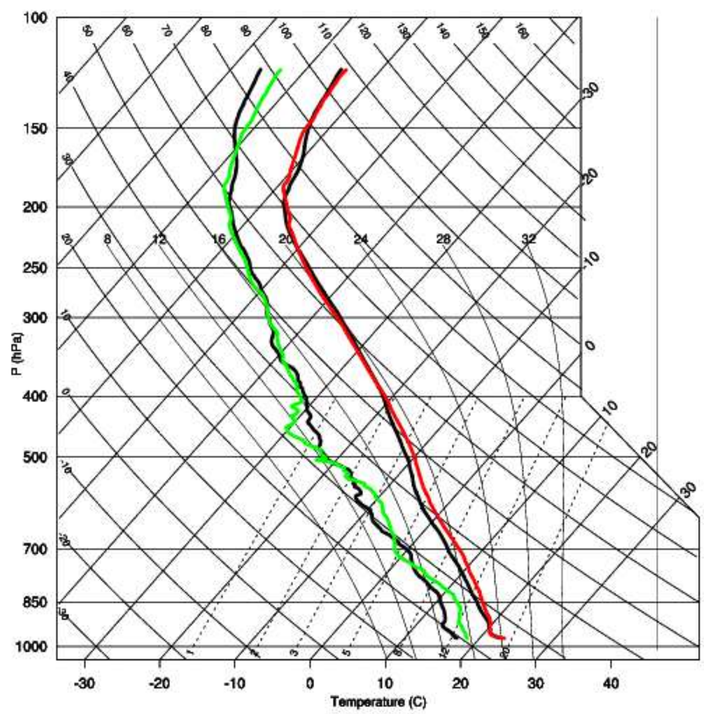

Figure 2: Composite skew-T log$p$ diagram for mean soundings in the upstream environment for crossing (colored) and noncrossing (black) cases.

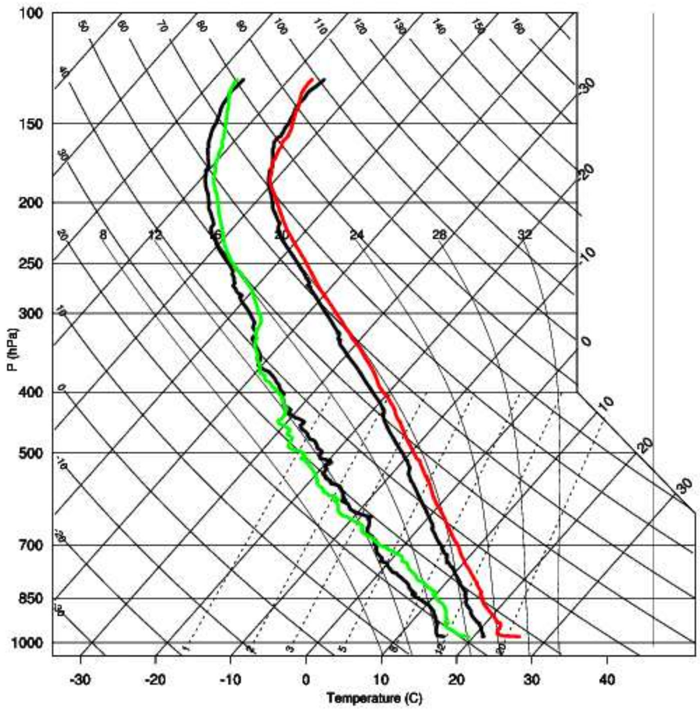

Figure 3: As in Figure 2, but for the downstream environment.

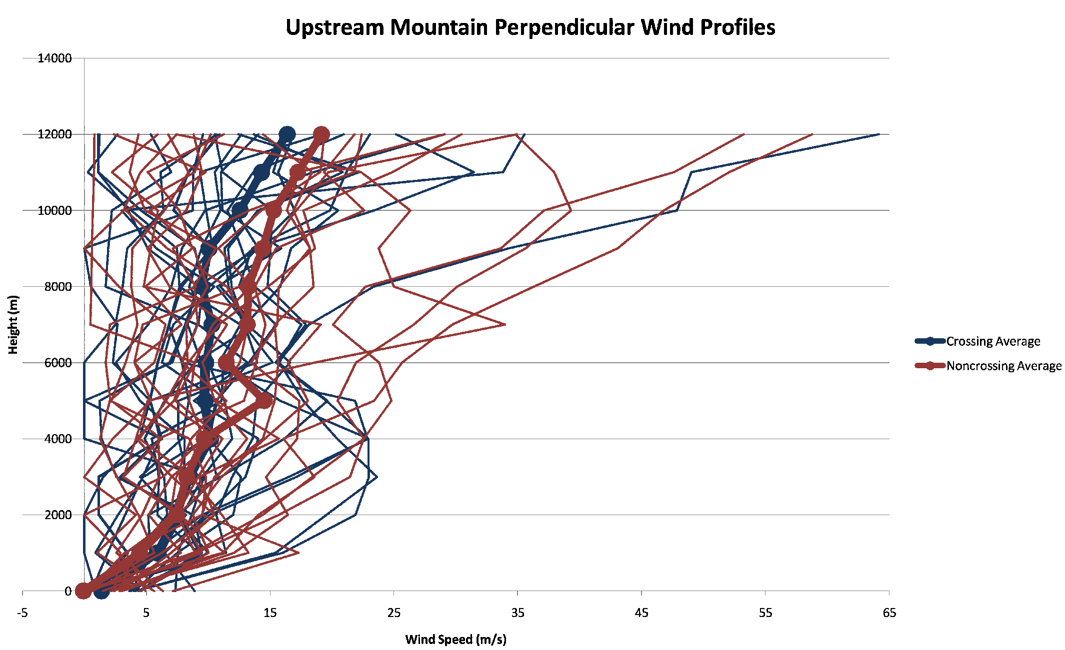

Figure 4: Mountain-perpendicular wind profiles for all of the crossing (blue) and noncrossing cases (red) in the upstream environment. The bold lines with markers indicate the average wind profile for each case type.

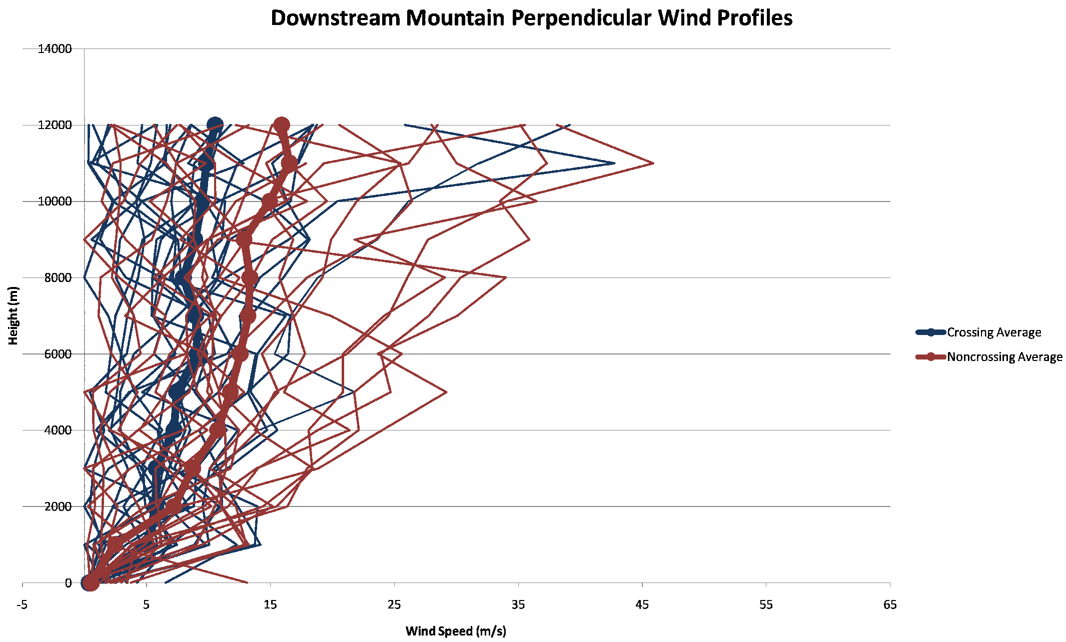

Figure 5: As in Figure 4, but for the downstream environment.

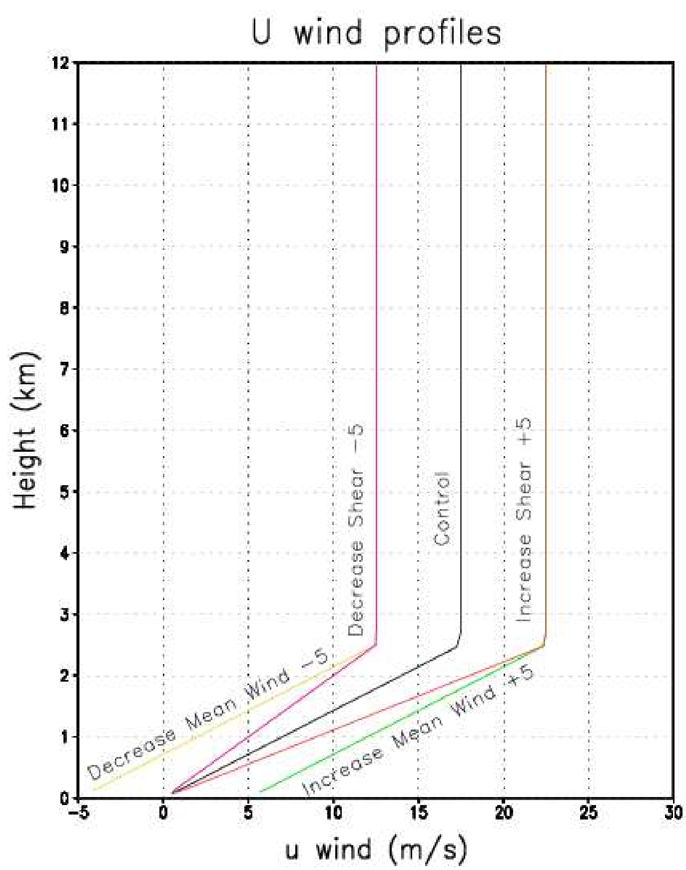

Figure 6: U-wind profiles used in the idealized numerical simulations.

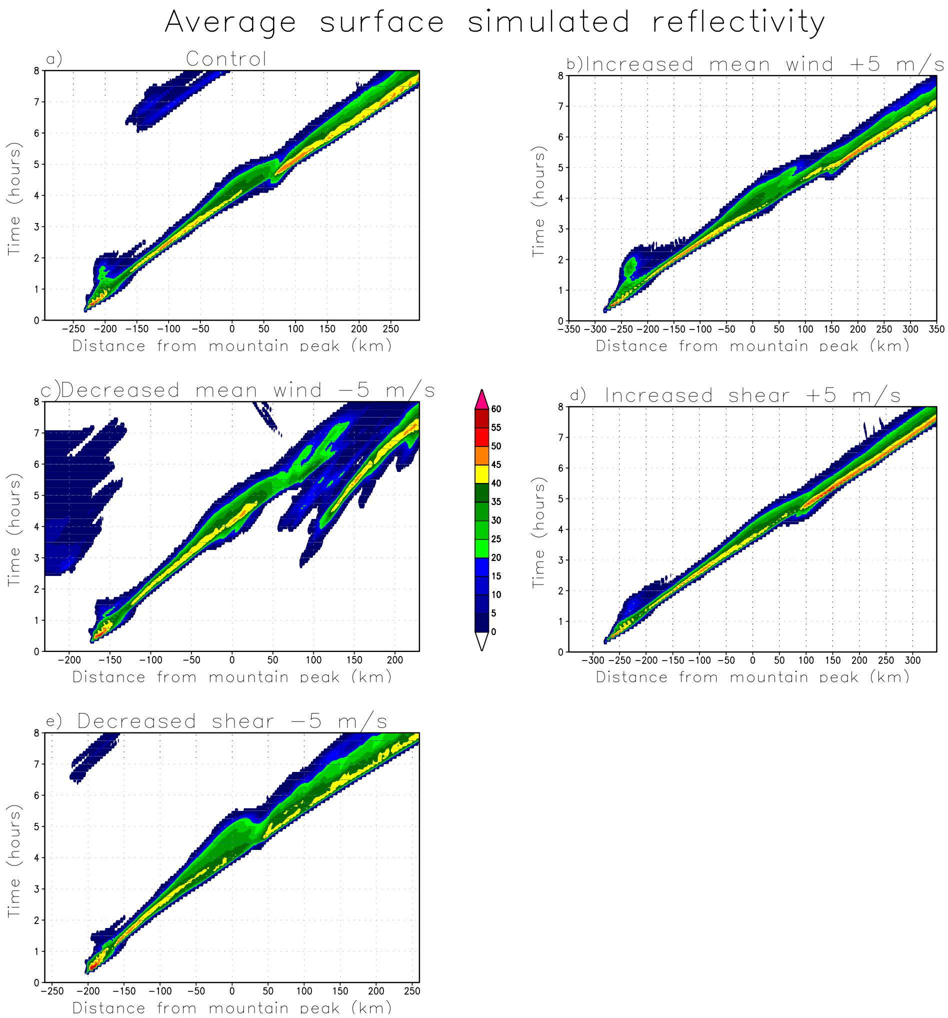

Figure 7: Hovmoller diagrams of along-line averaged surface reflectivity for the idealized simulations with the a) control, b) increased mean wind + 5 ms^{-1}, c) decreased mean wind -5 ms^{-1}, d) increased shear + 5 ms^{-1}, and e) decreased shear -5 ms^{-1} wind profiles. Time in hours is the y-axis, and distance from the mountain peak (at x=0) in km is the x-axis.

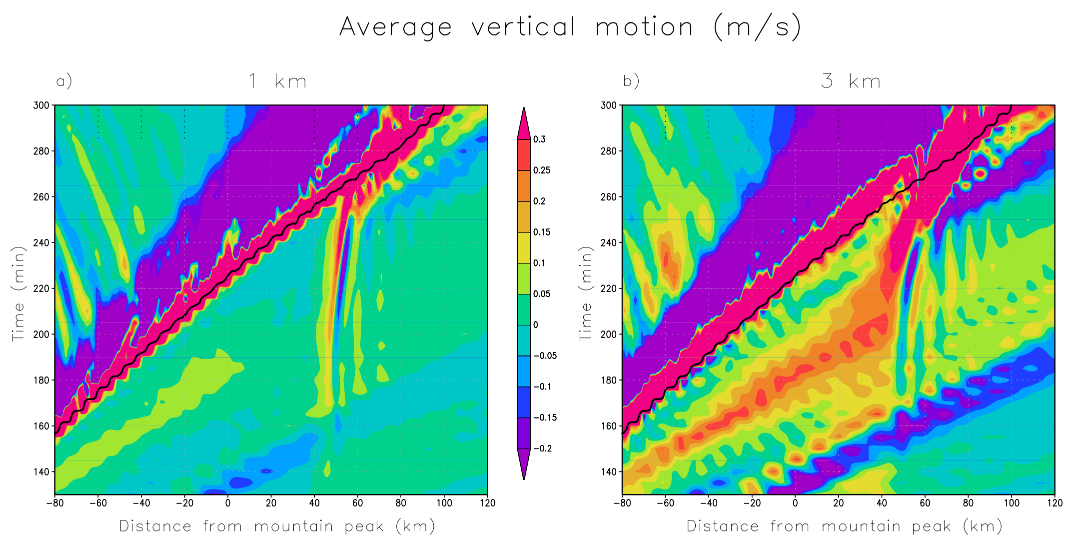

Figure 8: Hovmoller diagrams of the averaged vertical velocity (ms^{-1}) for the control simulation with terrain at a) 1 km and b) 3 km. The thick black line denotes the position of the outflow boundary as indicated by the θ'= -2 K contour.

Parameter	Crossing Average	Noncrossing Average	p-value
DCAPE (J/kg)	-688.6	-509.6	0.024140
MUCIN (J/kg)	-7.4	-26.6	0.077949
Mtn-perpendicular 0-6 km Shear (m/s)	7.7	11.0	0.089889
Maximum Bulk Shear (m/s)	23.1	29.8	0.124039
MLCAPE (J/kg)	963.0	464.9	0.130819
0-3 km Shear (m/s)	11.7	14.8	0.136659
2-8 km Shear (m/s)	12.8	18.2	0.145909
0-1 km Shear (m/s)	9.4	12.0	0.156688
0-6 km Shear (m/s)	13.1	18.3	0.207448
1 km Wind Speed (m/s)	12.1	14.5	0.267787
850 mb θ_e (K)	336.8	332.3	0.271777
MUCAPE (J/kg)	2068.5	1437.9	0.285007
3-12 km Mean Wind Speed (m/s)	17.8	21.3	0.282637
850 mb Dewpoint (^{o}C)	12.7	11.1	0.302427
Mtn-perpendicular Maximum Bulk Shear (m/s)	15.7	19.4	0.303237
Mtn-perpendicular Mean 3-12 km Wind Speed (m/s)	11.2	13.5	0.34917
Mtn-perpendicular 0-1 km Shear (m/s)	6.1	6.9	0.389006

Table 1: Parameter averages and p-values for the upstream environment. Only parameters whose p-value is < 0.4 is shown.

Parameter	Crossing Average	Noncrossing Average	p-value
SB CAPE (J/kg)	2403.9	518.9	0.000230
MUCAPE (J/kg)	2712.9	903.3	0.000260
Surface-500 mb θ_e Difference (K)	18.3	6.1	0.001410
0-3 km Lapse Rate (K/km)	7.0	5.5	0.002520
Maximum Bulk Shear (m/s)	20.1	30.2	0.003130
0-3 km Shear (m/s)	9.3	15.7	0.003170
3-12 km Mean Wind Speed (m/s)	12.8	21.1	0.003350
0-6 km Shear (m/s)	12.5	19.6	0.005140
Surface θ (K)	301.2	296.8	0.011200
Surface θ_e (K)	343.8	331.9	0.013150
LCL Height (m AGL)	866.2	521.5	0.017590
Mtn-perpendicular 0-3 km Shear (m/s)	5.7	9.3	0.018090
Surface Mixing Ratio (g/kg)	15.2	12.6	0.021470
Mtn-perpendicular Mean 3-12 km Wind Speed (m/s)	8.7	13.3	0.032580
MUCIN (J/kg)	-22.6	-62.8	0.046850
Mtn-perpendicular Maximum Bulk Shear (m/s)	13.9	19.4	0.055389
MLCAPE (J/kg)	593.8	317.7	0.056579
Mtn-perpendicular 0-6 km Shear (m/s)	8.5	11.6	0.100569
2-8 km Shear (m/s)	11.3	16.1	0.146079
SB CIN (J/kg)	-53.5	-104.1	0.228498
MLCIN (J/kg)	-69.2	-64.8	0.333607
850 mb Dewpoint (^{o}C)	11.4	10.1	0.354216

Table 2: As in Table 1, but for the downstream environment.